TECTONICS, VOL. 23, TC2006, doi:10.1029/2002TC001476, 2004

Normal faulting at convergent plate boundaries: Mylonitic extensional fabrics in the Franciscan subduction complex in Del Puerto Canyon, California, revisited

Uwe Ring and Peter P. Richter

Institut für Geowissenschaften, Johannes Gutenberg-Universität, Mainz, Germany

Received 4 November 2002; revised 11 November 2003; accepted 16 January 2004; published 13 March 2004.

[1] Using a strain and rotation analysis we tested the hypotheses that top-east mylonitic extensional structures in the uppermost Franciscan subduction complex in Del Puerto Canyon, California, accomplished exhumation of the Franciscan blueschists. We found no evidence of strongly noncoaxial deformation, instead our data indicate overall coaxial deformation in the proposed zone of mylonitic extensional deformation. There are no extensional strains, moderate vertical shortening occurred without horizontal extension and was compensated by modest deformation-related volume loss. There is also no strain gradient toward and within the proposed shear zone. Therefore the results of our work indicate that mylonitic extensional structures in Del Puerto Canyon do not exist. Overall, we conclude that there is no currently identifiable structure adjacent to or within the Franciscan in California that could have accommodated large-scale horizontal extension. Exhumation of the Franciscan blueschists was mainly achieved by erosion of an emergent forearc high. Our strain results and published data are also inconsistent with the development of a supercritically tapered Franciscan wedge that ultimately should have triggered normal faulting. Strain magnitudes are low despite the relatively long residence time of the rocks in the accretionary wedge. From this we infer that strain rates were low and that the wedge material flowed with a relatively high viscosity. Therefore ductile flow probably was not fast enough to form a supercritically tapered Franciscan wedge. *INDEX TERMS:* 8150 Tectonophysics: Plate boundary—general (3040); 8110 Tectonophysics: Continental tectonics—general (0905); 8015 Structural Geology: Local crustal structure; 8030 Structural Geology: Microstructures; *KEYWORDS:* deformation, volume loss, shear zone, normal faulting, accretionary wedge, Franciscan subduction complex California. **Citation:** Ring, U., and P. P. Richter (2004), Normal faulting at convergent plate boundaries: Mylonitic extensional fabrics in the Franciscan subduction complex in Del Puerto Canyon, California, revisited, *Tectonics*, *23*, TC2006, doi:10.1029/2002TC001476.

0278-7407/04/2002TC001476$12.00

1. Introduction

[2] The development of synorogenic normal faults in subduction-related accretionary wedges remains a controversial topic in tectonics. Large-scale synorogenic (or synsubduction) normal faulting has been proposed for the Franciscan subduction complex (or Franciscan for short) [*Platt*, 1986; *Harms et al.*, 1992] and from the forearc of the Cenozoic to Recent Hikurangi subduction zone in the North Island of New Zealand [*Pettinga*, 1982; *Walcott*, 1987]. In the latter case, local extension is accommodated by listric normal faults but the magnitude of extension is very small (1–5%) [*Cashman and Kelsey*, 1990] and thus insignificant. Horizontal extension in both accretionary complexes is attributed to underplating in the subduction zone and the development of a supercritically tapered wedge [*Platt*, 1986; *Walcott*, 1987; *Harms et al.*, 1992]. The well-studied Olympic subduction complex at the North American west coast shows no evidence for synsubduction normal faulting [*Brandon et al.*, 1998]. In the Mesozoic Torlesse accretionary wedge in the South Island of New Zealand, normal faults occur but they have been related to postsubduction rifting [*Deckert et al.*, 2002]. Nonetheless, large-scale synorogenic normal faulting is a widely established feature at forearc highs above retreating subduction zones and the Island of Crete in the Aegean is a well-known example [*Fassoulas et al.*, 1994; *Thomson et al.*, 1999; *Ring et al.*, 2001a]. This brief review shows that the Franciscan plays a critical role for tectonic concepts envisioning large-scale synorogenic normal faulting at nonretreating plate boundaries.

[3] *Platt* [1986] proposed that normal slip on the presently subvertical Coast Range fault zone above the Franciscan subduction complex (Figure 1) was responsible for the exhumation of the high-pressure metamorphic interior of the Franciscan. Normal slip at the Coast Range fault zone is supposed to be due to sustained collapse of a supercritical Franciscan wedge, i.e., that the wedge slope became too steep to be maintained by the basal shear stress. The Coast Range fault zone is the only candidate structure for exhumation of the Franciscan high-pressure rocks by normal faulting. The principal evidence for extensional faulting is as follows:

[4] 1. There is a major hiatus in metamorphic grade across the Coast Range fault zone, which places very low-grade rocks of the overlying Coast Range Ophiolite and Great Valley forearc basin against high-pressure rocks of the Franciscan [*Platt*, 1986].

[5] 2. The Coast Range Ophiolite, which lies above and contains the Coast Range fault zone, appears to have been vertically thinned at the same time [*Platt*, 1986; *Jayko et al.*, 1987].

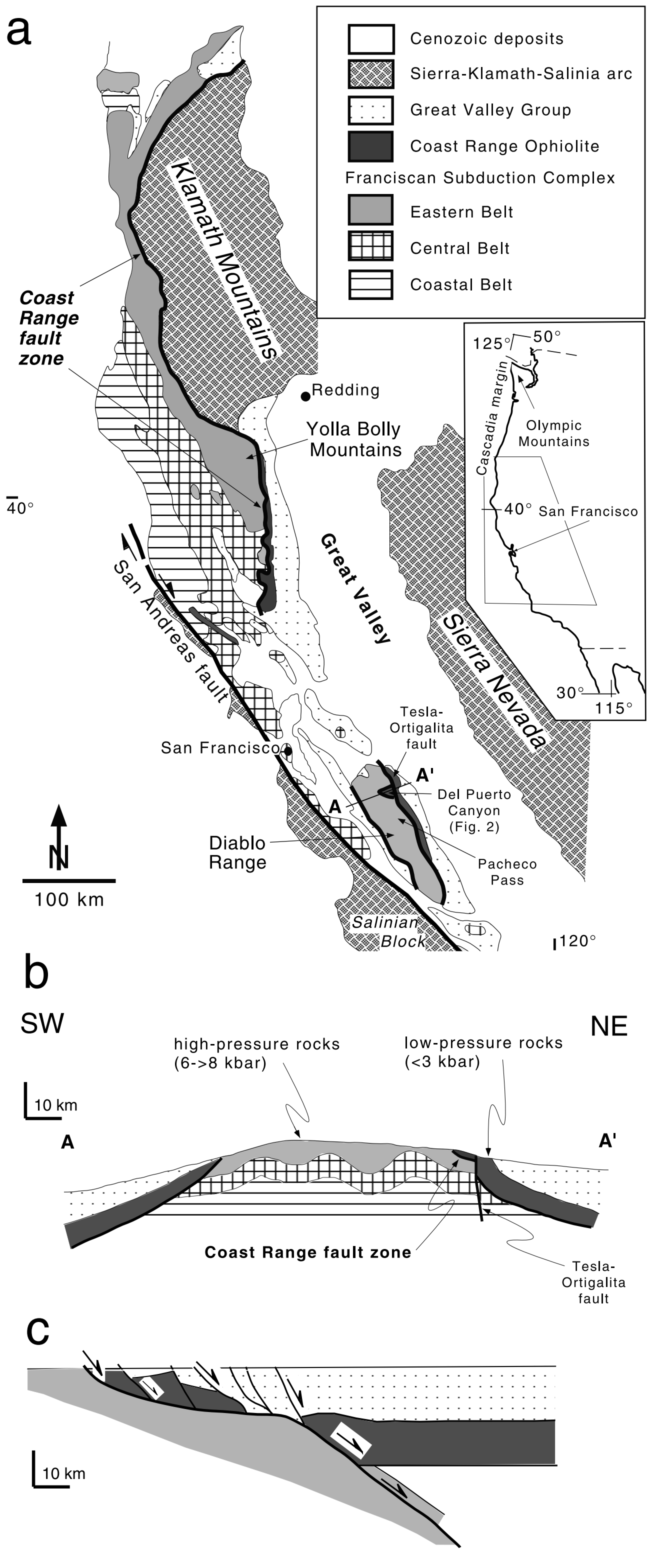

[6] 3. Kinematic evidence from Del Puerto Canyon in the Diablo Range has been interpreted to show top-east normal slip across the Coast Range fault zone [*Harms et al.*, 1992].

[7] The first two arguments are inconclusive because out-of-sequence thrusts can also result in younger-over-older relationships and can attenuate metamorphic section [*Boyer and Elliott*, 1982; *Wheeler and Butler*, 1993, 1994; *Ring*, 1995; *Ring et al.*, 1999]. Furthermore, available kinematic data from the Coast Range fault zone are not consistent with the proposed normal-slip interpretation [*Ring and Brandon*, 1994]. East of the Yolla Bolly Mountains in northern California and at the eastern flank of the Diablo Range in central California (Figure 1), the maximum-shortening axis of brittle strain is oriented near the down-dip direction of the fault zone and the overall sense of shear is top west. These data have been interpreted by *Ring and Brandon* [1994] to indicate that the Coast Range fault zone formed as a postmetamorphic out-of-sequence thrust with a general top-west sense of motion. In this respect it is important to note that pronounced differences in metamorphic grade between adjacent units of the underlying Franciscan and brittle strain data indicate that the present pattern of thrust imbrication within the Franciscan also postdated high-pressure metamorphism [*Suppe*, 1973; *Cowan*, 1974; *Platt*, 1975; *Worrall*, 1981]. Further evidence for top-west thrusting in the Coast Ranges comes from the Great Valley forearc west of the Yolla Bolly Mountains. *Glen* [1990] showed widespread evidence for postmetamorphic out-of-sequence thrusts that fit well with analyses of seismic reflection data, which have led to current models for tectonic wedging of the eastern Franciscan [*Wentworth et al.*, 1984; *Unruh et al.*, 1991, 1995; *Jachens et al.*, 1995]. An important conclusion is that evidence for normal faulting is largely lacking and may, therefore, not have played a major role for the exhumation of Franciscan blueschists. However, it should be pointed out that *Constenius et al.* [2000] criticized the tectonic wedging model and interpreted the seismic reflections to be related to synsedimentary normal faults, depositional onlap and a major structural-stratigraphic discontinuity. These authors suggested Jurassic-Cretaceous top-northwest normal faulting at the contact between the forearc massif and the Franciscan in northern California.

[8] *Harms et al.* [1992] argued that because of its low-angle geometry the Coast Range fault zone in Del Puerto

Figure 1. (a) Geologic map showing main Mesozoic tectonic elements of western California (see insert for location of map at North American west coast); our study area is located in Del Puerto Canyon of Diablo Range; also shown are localities referred to in text and location of Figure 2. (b) Generalized cross section through northern Diablo Range (A-A′, after *Bauder and Liou* [1979]); note break in metamorphism across Coast Range fault zone. (c) Extensional model explaining contact of Franciscan subduction complex and Great Valley Group by latest Cretaceous to Paleocene top-east normal faults (modified from *Harms et al.* [1992]).

Canyon is a remnant of the originally subhorizontal Coast Range fault zone. *Harms et al.* [1992] reported a pronounced deformation gradient in the uppermost 10 m of Franciscan sandstone directly underneath the Coast Range Ophiolite and proposed the existence of a mylonite zone, which we name the Del Puerto Canyon shear zone, in the uppermost Franciscan. *Harms et al.* [1992, Figure 3] stated that in this high-strain zone "mylonitic lineations" developed. Asymmetries of an anastomosing solution-mass-transfer cleavage were compared to S-C fabrics as defined for crystal-plastically deformed mylonite by *Berthé et al.* [1979] and were interpreted as indicating latest Cretaceous-Paleocene top-east extensional shear in the Del Puerto Canyon shear zone and, by inference, on the Coast Range fault zone itself (Figure 1). The timing of extensional shear and the suggested shear sense is in contrast to that proposed by *Constenius et al.* [2000]. *Harms et al.* [1992] did not report finite-strain or rotation data to support their interpretation of a high-strain zone and that the strain regime in this extensional shear zone was close to simple shear and that, therefore, the lineations are diagnostic of tectonic transport. The *Harms et al.* [1992] data are an important piece of evidence for normal faulting in the Franciscan. Hence, the proposed Del Puerto Canyon shear zone is very critical for tectonic models of the Franciscan and in more general terms for models indicating large-scale extension in subduction-related accretionary wedges at nonretreating plate boundaries.

[9] A deformation (strain and rotation) analysis is needed to demonstrate that the structures reported by *Harms et al.* [1992] were in fact formed by simple-shear deformation and are indicative of crustal extension. Therefore we have mapped the Del Puerto Canyon shear zone at the 1:10,000 scale and collected samples from Franciscan sandstone, especially from the uppermost 10 m of Franciscan strata (Figure 2), for a detailed strain and rotation analysis in order to test the interpretation of *Harms et al.* [1992]. Our data show that there is no high-strain zone or strain gradient in the uppermost Franciscan rocks and our rotation analysis is not compatible with top-east extensional shear.

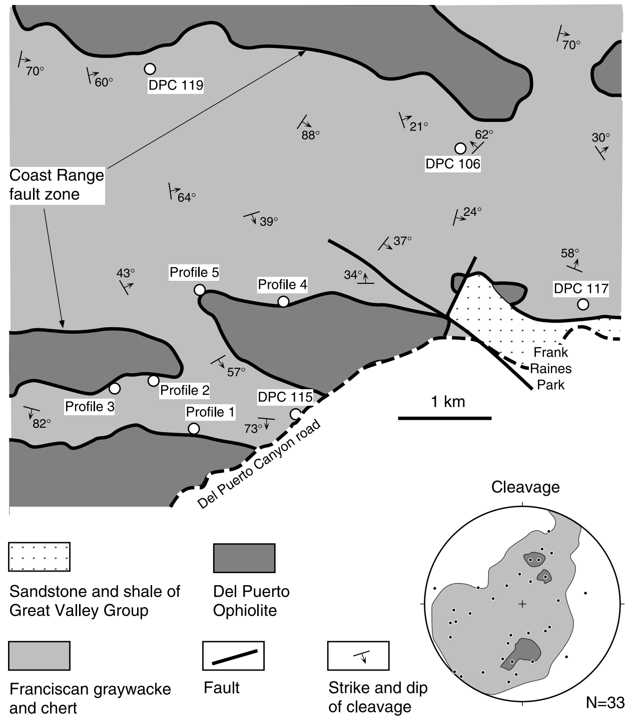

Figure 2. Geologic map of Del Puerto Canyon, representative strike and dip for Franciscan rocks, and locations of sampling profiles in uppermost 10 m of Franciscan subduction complex and of other samples; note relatively steeply dipping Franciscan rocks below generally flat-lying contact with Del Puerto Ophiolite. Stereogram shows poles to cleavage for Franciscan sandstone; contours were determined using method of *Kamb* [1959] and are in multiples of expected density for a uniform distribution; lowest contour is at 0.66 and interval for succeeding contours is 0.66.

2. Setting

[10] Most of California (Figure 1) is underlain by the Franciscan subduction complex, the Great Valley forearc massif, and the Sierran magmatic arc [e.g., *Cowan and Bruhn*, 1992]. The Coast Range fault zone juxtaposes the Franciscan with structurally higher rocks of the Jurassic Coast Range Ophiolite and the overlying Late Jurassic and Cretaceous Great Valley forearc basin [*Ingersoll*, 1978, 1979], which collectively represent the forearc massif that formed above and inboard of the Franciscan accretionary wedge.

[11] The Franciscan is dominated by clastic sedimentary rocks interpreted as accreted trench sediments and superimposed trench-slope basins. It also includes subordinate mafic and keratophyric volcanic rocks and thick chert sequences, which represent, at least in part, accreted fragments of seamounts and oceanic plateaus, as well as imbricated slices from the overlying Coast Range ophiolite. In the northern Coast Ranges, the Franciscan is commonly subdivided into three northwest-striking belts (Figure 1a), which are, from west to east: the Coastal, Central and Eastern Belts [*Irwin*, 1960; *Bailey et al.*, 1964; *Berkland et al.*, 1972; *Blake et al.*, 1988; *Wakabayashi*, 1992]. Stratigraphic age, as well as the degree and age of metamorphism and deformation, generally increase in an eastward direction across these belts. In the Diablo Range, the threefold subdivision is not as apparent and has been obscured by faulting associated with the modern San Andreas transform boundary. However, it is widely accepted that the Franciscan in the Diablo Range is analogous to the Eastern belt of the northern Coast Ranges [*Blake et al.*, 1988; *Harms et al.*, 1992].

[12] The Eastern Belt constitutes the uppermost part of the Franciscan (Figure 1). The term Eastern Belt is generally used to refer to a distinctive imbricated sequence of several thick, gently dipping, fault-bounded units, each of which contains a relatively coherent internal stratigraphy [*Suppe*, 1973; *Worrall*, 1981; *Blake*, 1981]. Metamorphic grade is blueschist facies as indicated by the widespread occurrence

of lawsonite, aragonite, glaucophane and jadeite [*Blake et al.*, 1988; *Ernst*, 1993]. Metamorphic conditions in the Diablo Range were 7 – >8 kbar and 100–200°C in the Pacheco Pass area [*Ernst*, 1993]. Regional high-pressure metamorphism in the Diablo Range occurred at about 92 Ma as indicated by U-Pb isotopic ages on sphene and plagioclase [*Mattinson and Echevirra*, 1980]. This age agrees well with K-Ar ages from intact graywacke [*Suppe and Armstrong*, 1972].

[13] Along both flanks of the Diablo Range, the Great Valley Group and remnants of the Coast Range Ophiolite occur. On the eastern flank, both units occur in a steeply east-dipping homocline. The Great Valley Group consists of the Jurassic Lotta Creek Tuff Member and the Knoxville Formation, overlain by the Late Cretaceous Panoche and Moreno Formations [*Maddock*, 1964; *Ingersoll*, 1979; *Bartow and Nilsen*, 1990]. The Coast Range Ophiolite and the lowermost units of the Great Valley Group show zeolite to incipient prehnite-pumpellyite facies metamorphism [*Dickinson et al.*, 1969] (Figure 1b).

[14] In general, the contact between the rocks of the Coast Range Ophiolite and the Franciscan in the eastern Diablo Range is the young, steeply dipping, dextrally displacing Tesla-Ortigalita fault [*Maddock*, 1964], which deformed the Coast Range fault zone. In Del Puerto Canyon, the Coast Range Ophiolite, locally referred to as the Del Puerto Ophiolite [*Evarts*, 1977], overlies the Franciscan with a subhorizontal fault, the original Coast Range fault zone [*Harms et al.*, 1992] (Figure 1b).

[15] Exhumation of the Eastern Franciscan Belt to shallow crustal levels occurred during the Late Cretaceous and Early Tertiary as indicated by apatite and zircon fission-track dating [*Dumitru*, 1989; *Tagami and Dumitru*, 1996], by the recognition of reworked blueschist-facies clasts in conglomerates thought to be deposited in Late Cretaceous trench-slope basins [*Cowan and Page*, 1975], and by unmetamorphosed Eocene strata resting unconformably upon Franciscan rocks [*Page and Tabor*, 1967].

[16] *Ring and Brandon* [1999] estimated that the residence time in the wedge, i.e., the time between initial accretion and final exhumation, was about 35 Myr for the rocks from the Diablo Range. On the basis of this timing information and the P-T data, an average exhumation rate of 0.8 km Myr^{-1} was estimated, which is comparable to modern rates determined for the Cascadia margin [*Brandon and Vance*, 1992].

3. Strain and Rotation Analysis

3.1. Field Observations and Sampling

[17] In the field, Franciscan sandstone shows a variably developed spaced solution-mass-transfer (SMT) cleavage. In most cases, preferred orientation of lithic fragments allows easy recognition of this planar fabric. However, sometimes the rocks show no obvious cleavage in the field. Linear fabrics were hardly visible in outcrop, only occasionally elongated lithic fragments define a weak lineation. The immediate contact between the uppermost Franciscan and the Coast Range Ophiolite, i.e., the proposed Del Puerto Canyon shear zone, is characterized by cataclastically reworked sandstone, which in part grades into gouge layers. Mesoscopically, the spaced cleavage in the sandstone does not become more closely spaced toward the tectonic contact. In places, the cleavage is cut by cataclasite and gouge layers, which have a distinct spatial and orientational relationship to the contact with the ophiolite. The SMT cleavage does not show any obvious spatial or orientational relationship with the contact to the ophiolite. Therefore the mesoscopic structures as observed in the field do not a priori support the existence of a ductile shear zone in the uppermost ~10 m of the Franciscan in Del Puerto Canyon.

[18] Sampling for the determination of finite-strain directions and for absolute finite-strain analysis was carried out in two different formats: (1) We collected 17 samples from five profiles within 10 m below the contact of the Franciscan high-pressure sandstone and the Del Puerto Ophiolite, i.e., we sampled the zone from which *Harms et al.* [1992] reported the mylonitic extensional structures. From these 17 samples only 11 were suitable for finite-strain analysis, the other six samples were too strongly altered. (2) We randomly collected another four samples from Franciscan sandstone where the rock types are homogeneous at the scale of sampling. These additional samples allow comparison of strain from the proposed mylonite zone with that from sandstone outside the proposed shear zone. Furthermore, the additional samples ensure to obtain a reliable tensor average for SMT deformation in Del Puerto Canyon. Because it has been proposed that the lithic fragments (Figure 3a) took up most of the ductile deformation, we carried out a R_f/ϕ analysis on three samples containing lithic fragments (two of these three samples are from northern California) to see whether the lithic fragments, in general, record higher strain than the sandstone matrix.

3.2. Microstructures

[19] Our strain methods are designed for measuring strain and rotation in rocks deformed by SMT processes. In this context, we assume that all strain occurs by changes at the boundaries of grains, and that intragranular strains are negligible. We support this assumption with a detailed discussion of the deformation textures.

[20] The units we sampled are dominated by siliciclastic sandstones, with quartz and feldspar as the dominant detrital phases [*Dickinson et al.*, 1982]. Petrographic evidence indicates that SMT was the dominant deformation mechanism operating in the sandstone samples from Del Puerto Canyon. These sandstones are in part composed of first-cycle volcanogenic sediment. Monocrystalline grains of volcanic quartz and plagioclase show little to no undulose extinction, deformation laminae, or deformation twinning. Polycrystalline quartz grains do show undulose extinction and other evidence for intracrystalline deformation. These grains are interpreted to be metamorphic detritus because intracrystalline deformation is limited to these grains and because their microstructures lack systematic orientations. This conclusion is further supported by the fact that the metamorphic grains are commonly mantled by fiber overgrowths, which do not show intracrystalline deformation

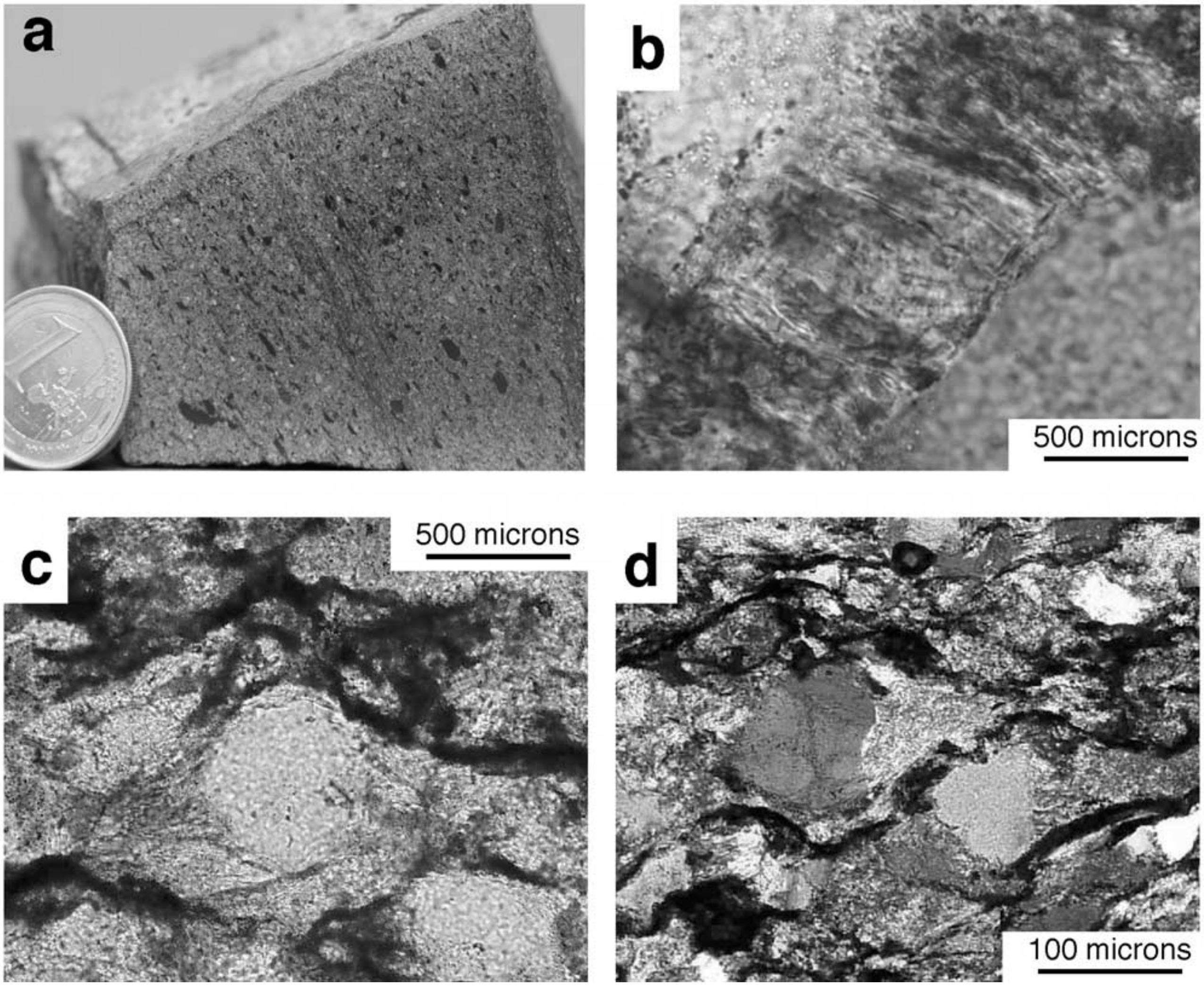

Figure 3. (a) Lithic fragments in XZ section of sandstone defining cleavage; note that aspect ratios of fragments show wide scatter; sample 93–27a (see *Ring and Brandon* [1999] for sample locality). (b–d) Microphotographs of typical XZ sections from Franciscan sandstone in Del Puerto Canyon. (b) Crossed-polarized image of straight fibers between quartz grains; sample P2/2. (c) Tapered and slightly curved fiber bundles behind quartz; sample P4/1. (d) Tapered fiber bundles behind quartz; crossed-polarized light; sample P4/1. See color version of this figure in the HTML.

(Figures 3b–3d). The dominance of the SMT mechanism is consistent with metamorphic temperatures, which were everywhere well below the ~300°C threshold needed to activate dislocation glide-and-climb in quartz [*Küster and Stöckhert*, 1997].

[21] Quartz and feldspar are truncated by thin selvages composed of insoluble minerals (Figures 3c and 3d). The selvages can be regarded as planes of finite flattening that formed perpendicular to Z (X, Y and Z refer to the maximum extension, intermediate and maximum principal strain directions [*Ramsay and Huber*, 1983]). Directed fibrous overgrowths of quartz, chlorite, and white mica mantle those grain boundary segments at a high angle to cleavage. The fiber overgrowths are considered to record extensional strains that accumulated during SMT deformation.

[22] In XZ sections, the fiber bundles generally lie subparallel to the trace of cleavage (Figure 3b). Individual fiber bundles typically have a tapered geometry, with fibers converging away from the host grain. This tapered geometry is recorded in the distribution of fiber directions, which commonly vary by as much as ±15° around the average direction. The taper geometry has been explained as resulting from dissolution between the fibers to accommodate shortening in the Y and Z directions (semi-deformable antitaxial fiber model of *Ring and Brandon* [1999]). Extension parallel to X is accommodated solely by growth of new fibers, a conclusion that is corroborated by cathodoluminiscence work [*Ring*, 1996]. The fibers are inferred to accrete at the grain boundary, so that the amount of shortening across the fibers is largest at the end of the bundles. This explanation accounts for the observation that the degree of

tapering seems to increase with the amount of shortening in the section. For instance, fiber bundles are more tapered in XZ sections than in XY sections because shortening is greater in Z than in Y.

[23] We assume that the fibers track the incremental X direction during the deformation history of the rock, whereas cleavage records the XY plane for total SMT strain. Thus parallelism between fibers and cleavage indicates a coaxial deformation [*Feehan and Brandon*, 1999; *Ring and Brandon*, 1999; *Ring et al.*, 2001b]. As noted above, most of our samples have fibers that parallel the trace of cleavage. However, some samples have an average fiber orientation in the XZ section that is oblique to the trace of cleavage, indicating noncoaxial deformation. In a few samples, we found individual fibers with an obliquity of up to 10–30° to cleavage. Nonetheless, the average angle between fibers and cleavage in these samples is less than 10°.

[24] The fact that newly crystallized material consists of directed fibers shows that there was little or no porosity during SMT deformation. All of the space between grains is presently occupied by selvages or directed fiber overgrowth. Dissolution along selvage surfaces would quickly remove an initial porosity. Transient porosity might have existed along the incoherent surfaces that separated the fiber overgrowths from their host grains. However, the porosity along this surface would have been small given that displacement-controlled fiber overgrowths only form when crack apertures are small, on the scale of microns or less [*Fisher and Brantley*, 1992]. We suggest that mechanical compaction had already removed much of the primary porosity before the onset of SMT deformation. This result would be expected for a poorly sorted sediment where grains of different sizes could be compacted into a tightly packed aggregate.

[25] *Ernst* [1965, 1987, 1993] reported detailed metamorphic textures from Franciscan sandstone of the Diablo Range. Coarsely crystalline, concentrically and oscillatorily zoned jadeite prisms replace host grains of plagioclase + quartz. Tiny, fibrous jadeite overgrowths that grew on larger jadeite grains extend into the sandstone matrix and possess the same chemical composition as the jadeite host [*Ernst*, 1992]. Euhedral jadeite and aragonite occur in quartzose veins. Sodic amphibole occupies stringers and fracture-related patches. Our observations in the Pacheco Pass area show that extensional veins that crosscut a semi-penetrative SMT cleavage contain coarse-grained jadeite. Microprobe analyses revealed that the directed fiber overgrowths associated with SMT deformation are composed of quartz, muscovite, phengite, chlorite and lawsonite. The Si content of the phengite is between 3.49 and 3.51 per formula unit [*Ring*, 1996].

[26] The high Si content of phengite [*Massone and Schreyer*, 1987] and the occurrence of lawsonite, aragonite and jadeite in veins and fibers demonstrate that SMT deformation commenced at the peak of high-pressure metamorphism. Thus we envision that SMT strain accumulated while the Franciscan rocks were accreted and moved through the wedge. As shown above, the out-of-sequence thrust faults within the Franciscan postdated regional high-pressure metamorphism and are late-stage structures. Therefore SMT deformation predated the out-of-sequence thrusts, i.e., the out-of-sequence thrust faults cut the metamorphic section at a relatively high crustal level and cataclastically reworked SMT fabrics. Our observations indicate that fibrous overgrowth was the sole mechanism of precipitation during SMT deformation.

3.3. Methods of Deformation Analysis

[27] Our study employs the PDS (Projected Dimension Strain), Mode, and Fiber methods for measuring absolute strain and internal rotation in sandstones deformed by the SMT mechanism [*Brandon et al.*, 1994; *Ring and Brandon*, 1999]. In our discussion here, the principal stretches are designated as $S_X > S_Y > S_Z$, where S = final length/initial length. Measurements were made using XY and XZ thin sections.

[28] The PDS method is used to measure the average shortening produced by dissolution of grain boundaries. The method exploits the fact that for SMT deformation, the dimensions of the detrital quartz and feldspar grains remain unchanged in the X direction (i.e., deformation is intergranular, not intragranular). Therefore the grain diameter in the X direction provides a record of the original size of the grain and thus an absolute reference frame. The central idea behind the PDS method is that parallel to principal directions with $S < 1$, SMT deformation has reduced the average dimension of the detrital grains by a factor equivalent to the principal stretch. In contrast, the average initial dimension of a detrital grain should be preserved in the X direction because the grains lack any significant internal deformation and because the original grain surface is mantled by fiber overgrowths. Therefore a contractional principal stretch can be determined by finding the average grain dimension parallel to a contractional principal direction and dividing it by the average grain dimension parallel to X. Dimensions are measured in a two-dimensional thin section, so a correction is needed to get the appropriate three-dimensional result [*Feehan and Brandon*, 1999].

[29] Our measurements were made using a petrographic microscope with a camera lucida tube and digitizing tablet. Measurements are precise to better than ±3 microns. The dimensions of each grain are represented by their caliper dimensions (or projected dimensions) in the principal directions lying in the section. The caliper dimensions of the grains are not affected in any significant way by grain rotations associated with compaction. For instance, PDS measurements on undeformed sandstones gave undeformed results (i.e., $S \sim 1$) [*Ring and Brandon*, 1999].

[30] The Mode method is used to determine the extensional strain recorded by the fiber overgrowths. The modal percentage of fibers in a rock is directly related to the absolute extensional stretch in the rock. Fiber modes are most easily measured in the XZ section. For unidirectional fibers, $S_X = (1\text{-m})^{-1}$, where m is the modal fraction of fiber.

[31] Given absolute strains, the volume stretch S_V (= final volume/initial volume) is equal to the product of the principal stretches ($S_X \times S_Y \times S_Z$). Because our methods

Table 1. Measurements of SMT Deformation From Del Puerto Canyon[a]

Sample	Stretches				Axial Ratios				Directions (Trend/Plunge)			Rotation W^*_m	Shear Sense
	S_X	S_Y	S_Z	S_V	R_{XY}	R_{YZ}	R_{XZ}	Γ_{oct}	X	Y	Z		
P1/1	1.16	1.01	0.79	0.92	1.15	1.28	1.47	0.31	303/52	103/36	200/10	1.54	top-ESE
P1/2	1.16	0.97	0.86	0.97	1.20	1.13	1.35	0.24	334/18	231/34	86/50	nd	nd
P1/3	1.24	1.00	0.86	1.06	1.24	1.16	1.44	0.30	123/35	234/24	350/45	0.43	top-NW
P2/2	1.37	0.98	0.75	1.00	1.40	1.31	1.83	0.49	171/40	52/30	297/36	0.19	top-NNW
P2/3	1.22	1.00	0.93	1.13	1.22	1.08	1.31	0.22	82/38	315/38	199/30	0.67	top-E
P3/3	1.11	0.92	0.88	0.89	1.21	1.05	1.26	0.19	198/16	301/40	91/46	nd	nd
P3/4	1.10	0.86	0.86	0.80	1.28	1.00	1.28	0.20	73/77	206/9	297/9	nd	nd
P4/1	1.25	1.00	0.79	0.99	1.25	1.27	1.58	0.37	90/60	270/30	360/0	0.17	top-E
P4/3	1.26	1.06	0.89	1.19	1.19	1.19	1.42	0.28	200/4	291/13	91/76	1.00	top-ENE
P5/1	1.16	1.03	0.87	1.04	1.13	1.18	1.33	0.23	100/3	190/11	355/79	0.57	top-SE
P5/2	1.08	1.00	0.84	0.91	1.08	1.19	1.29	0.20	148/48	54/4	320/42	nd	nd
Tensor average for proposed mylonite zone in Del Puerto Canyon	1.05	0.99	0.95	0.99	1.06	1.04	1.11	0.08	127/43	226/10	327/45	0.71	top-NW
DPC106	1.08	1.02	0.65	0.72	1.06	1.57	1.66	0.41	142/26	32/36	266/45	nd	nd
DPC115	1.22	0.97	0.75	0.89	1.26	1.29	1.63	0.40	176/17	81/15	313/67	0.25	top-SSE
DPC117	1.21	1.08	0.91	1.19	1.12	1.19	1.33	0.23	60/53	304/19	202/31	nd	nd
DPC119	1.02	0.95	0.83	0.80	1.07	1.15	1.23	0.17	165/72	333/18	64/3	nd	nd
Tensor average for all data	1.04	0.96	0.93	0.93	1.08	1.03	1.12	0.09	141/45	50/0	320/45	0.51	top-NW

[a]Samples Px/x are from profiles within uppermost 10 m of Franciscan, i.e., from proposed extensional mylonite zone in Del Puerto Canyon (sample P1/x is from profile 1; sample Px/1 is closest to overlying Del Puerto Ophiolite); nd, not determined.

focus entirely on the loss of mass from grains and the amount of mass locally precipitated, our estimates of S_V only represent the mass-transfer component of the volume strain. Other sources of volume strain include changes in porosity and mineral density. Porosity is thought to have been small at the start of SMT deformation and is thus ignored. Changes in mineral density are insignificant at the low metamorphic grade in our study area.

[32] The geometric relationship between the fiber overgrowths and the trace of cleavage was used to estimate the internal rotation associated with SMT deformation [*Ring and Brandon*, 1999]. The basic idea is that the fiber overgrowths track the incremental extension direction during deformation, whereas cleavage approximates the XY plane of finite deformation. Internal rotation was estimated using the FIBER program to model the shape of about 30–50 fibers digitized in the XZ section [*Ring and Brandon*, 1999]. The internal rotation axis is assumed to be parallel to Y.

[33] Table 1 reports the principal stretches and axial ratios and also the natural octahedral shear strain, Γ_{oct}, which is a measure of the average distortional strain caused by the deformation [*Nadai*, 1963; *Brandon*, 1995]. This measure is zero when $S_X = S_Y = S_Z$ and increases as R_{XY}, R_{YZ} and R_{XZ} increase. Also reported in Table 1 is the modified kinematic vorticity number, W^*_m of *Ring and Brandon* [1999], which accounts for volume strains and the sense of shear as deduced from the sense of curvature of the fibers with respect to cleavage. Definitions and other details are given by *Ring and Brandon* [1999]. The m subscript for the kinematic number indicates a path-averaged value assuming a steady three-dimensional deformation. The simple geometry of the overgrowths in our samples suggests that SMT deformation was fairly steady, at least in its orientation.

[34] Table 1 also reports tensor averages for our deformation measurements. As shown below, the directions for the principal stretches and the rotation axes generally do not show a strong degree of preferred orientation. The variability in orientations probably reflects local variations in deformation and also random errors in our measurements. *Feehan and Brandon* [1999] suggested that SMT deformation might be typified by local-scale variability, especially in the orientations of X and Y. Thus we have found it essential to calculate averages for these data, as has been done in other studies from regions with widely varying principal directions [*Feehan and Brandon*, 1999; *Ring and Brandon*, 1999; *Bolhar and Ring*, 2001; *Ring et al.*, 2001b; *Deckert and Brandon*, 2004]. This average strain tensor corresponds to the tensor that most closely represents the strain experienced by a material line that bounds the sampled region [*Cobbold*, 1977]. As discussed by *Brandon* [1995], deformation data must be averaged in tensor form to ensure that the magnitudes and directions of the principal stretches and rotations are correctly associated. If the rotational component of the deformation is small, then one can average the stretch tensor and the internal rotation tensor separately, without introducing significant errors [*Brandon*, 1995]. In this study, tensor averages were calculated using the Hencky method (see Appendix B of *Brandon* [1995]).

3.4. Data

[35] Figure 4 illustrates the changes of S_X, Γ_{oct} and W^*_m within the proposed Del Puerto Canyon shear zone. In general, these parameters show no increase toward the contact with the Coast Range Ophiolite. Strain and rotation is generally small and the finite-strain directions in the proposed Del Puerto Canyon shear zone show considerable

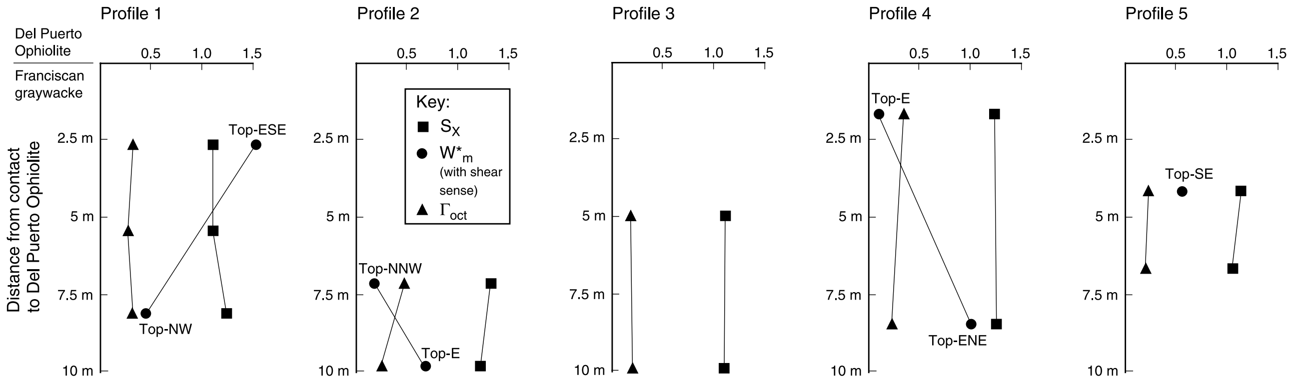

Figure 4. Profiles 1 to 5 depicting changes of S_X, Γ_{oct} and W^*_m with sense of rotation within proposed Del Puerto Canyon shear zone; note that W^*_m could not be determined for every sample; for locations of profiles refer to Figure 2.

scatter (Table 1). The variable sense of rotation is not compatible with top-east tectonic transport. Only in profile 2 there seems to be an increase in strain toward the contact with the Coast Range Ophiolite. However, this strain increase is modest and the sense of rotation in this profile shows no consistent pattern. Overall, it seems obvious that there are no gradients in strain and rotation, which are consistent with the existence of a top-east mylonite zone. The strikingly low strain magnitudes in the proposed shear zone are also well expressed by the small axial ratios, which range for XZ sections from 1.26 to 1.83. Moreover, the strain and rotation data from the proposed Del Puerto Canyon shear zone are not different from the strain measurements of the samples collected randomly from Franciscan sandstone in Del Puerto Canyon (Table 1). S_X and Γ_{oct} for instance vary between 1.08–1.37 and 0.19–0.49 in the proposed Del Puerto Canyon shear zone and for the other Franciscan samples S_X and Γ_{oct} vary between 1.02–1.22 and 0.17–0.41. The strain-tensor averages are also very similar (Table 1). Therefore the samples from the uppermost Franciscan are representative for regional strain in the Eastern Franciscan Belt and can be discussed with the other Franciscan data for exploring regional strain patterns.

[36] The field orientations of all measured finite-strain axes in Del Puerto Canyon scatter considerably (Figure 5 and Table 1). In general, cleavage has a moderate to steep dip. The contours for the poles to cleavage (Figures 2 and 5) in the rocks from Del Puerto Canyon depict folding about roughly east trending open folds. The pattern of Z axes from the strain measurements are somewhat different from the field measurements of cleavage as shown in Figure 2, which might be due to the relatively small number of strain measurements. The outcrop pattern of the Coast Range Ophiolite agrees with gentle folding about east trending axes. *Ernst* [1993] also described open folding with east trending axes from the Pacheco Pass area of the Diablo Range. Because of open folding, the plunge of the maximum extension direction is also variable but on average S_X plunges moderately to the east/southeast. Contouring of the data reveals a moderate inclination for X and Z and a subhorizontal attitude for Y. The principal directions of the average strain tensor (open symbols in Figure 5) yield similar results.

[37] The measurements of the modal abundance of fibers in the rock indicate that the sandstones contain between 2% and 27% fiber per volume of rock. Therefore the maximum extensional stretch, S_X, shows a relatively wide scatter in magnitude, ranging from 1.02 to 1.37. S_Z ranges from 0.65 to 0.93, and S_Y ranges from 0.86 to 1.08 with the data split evenly between slightly constrictional ($S_Y < 1$) and slightly flattening ($S_Y > 1$) strain types (Figure 6). The tensor average ($S_X : S_Y : S_Z = 1.04 : 0.96 : 0.93$) indicates that $S_X \approx 1$. This surprising result stems from the highly variable orientations of the principal finite strain axes; the individual strain tensors do not share the same principal directions. Because S_Y is also $\approx$1, the overall deformation at a regional scale is uniaxial flattening and plane strain, i.e., volume strain largely accounts for the modest shortening of 7%.

[38] Most analyzed samples have experienced volume loss ranging between 1% and 28%. Five samples show evidence for volume gain of 4% and 19%. Because the PDS and Fiber methods are designed to measure deformation of the grains, we conclude that the volume strain must have occurred by loss of mass from individual detrital grains. On average, the data indicate that 7% of the rock volume was lost during regional SMT deformation in Del Puerto Canyon. In Figure 6 all three principal stretches show a positive correlation with volume strain.

[39] The average kinematic vorticity number of the individual samples shows considerable scatter, but is, on average, small and the sense of rotation is variable (Table 1). Therefore we conclude that on the regional scale the average deformation was largely coaxial.

[40] R_f/ϕ analysis on the lithic fragments indicates that these fragments did not take up more strain than the quartz grains. When recalculated for the observed volume loss, the stretches from R_f/ϕ analysis of sample P3/4 from Del Puerto Canyon and samples 93–27a and 96–57 from northern California (see *Ring and Brandon* [1999] for sample localities) are not fundamentally different from those obtained with the PDS and Mode methods (Table 2). Likewise, Γ_{oct} as obtained from R_f/ϕ analysis of the lithic fragments is not significantly higher than Γ_{oct} for SMT strain. The general conclusion that the strain magnitude in the lithic fragments is similar to that for SMT strain is in agreement with the

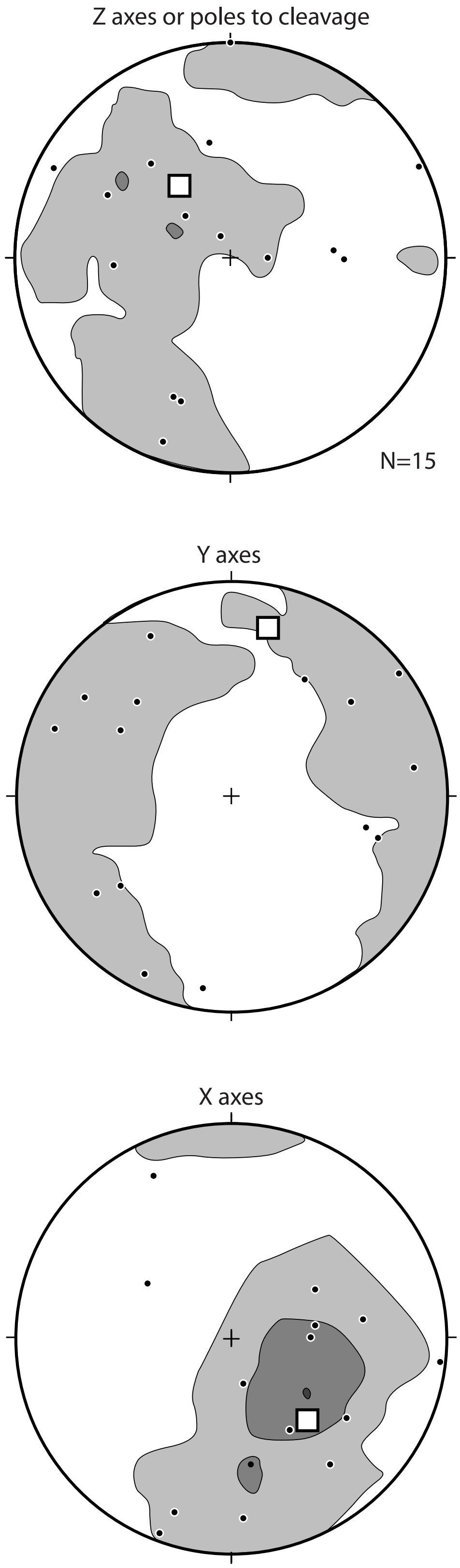

Figure 5. Lower hemisphere equal-area stereograms of finite-strain axes from Del Puerto Canyon; also shown are axes of tensor average (large open squares). Contours as in Figure 2.

results reported by *Deckert and Brandon* [2004] from the Torlesse accretionary wedge in New Zealand. These authors showed that finite strain as obtained by X-ray texture goniometry of phyllosilicates is of similar magnitude as those obtained from PDS and Mode analysis of quartz grains.

[41] An important aspect of volume strain is highlighted in Figure 6c, where isolines of aspect ratios in XZ sections (calculated for the plane-strain case) are projected into a diagram for the absolute strain values S_V and S_X. This diagram illustrates how volume and extensional strains relate to cleavage formation, if cleavage is assumed to be perpendicular to Z and the maximum axial ratio R_{XZ} is considered as a proxy for cleavage intensity. S_V and S_X can be regarded as the open and closed components of the deformational system. Therefore a strain path parallel to S_V would represent a pure volume strain, and a path parallel to S_X would characterize constant-volume (S_V = 1) plane-strain deformation, where extension in X is balanced by shortening in Z. The data points in Figure 6c do not plot on either of these strain paths, indicating that deformation apparently involved both closed- and open-system behavior. As shown by *Brandon* [1995], the closed-system case (S_V = 1) requires only half as much strain as the open-system case to produce the same R_{XZ} ratio. The aspect ratios in the samples are higher than would be expected given the low absolute stretches.

4. Discussion

4.1. Implications for the Proposed Del Puerto Canyon Shear Zone

[42] Our work on the mylonitic extensional fabrics in Del Puerto Canyon shows that there is no evidence for a mylonite zone in the uppermost Franciscan as advocated by *Harms et al.* [1992]. We have found no high strains and no evidence of strongly noncoaxial deformation. The strain does not increase toward and within the uppermost 10 m of Franciscan sandstone. The mapped maximum stretch directions depict a highly variable pattern and there is no evidence for a preferred sense of rotation in the uppermost Franciscan. A close inspection of Figure 3 of *Harms et al.* [1992] shows that our finding of variable senses of rotation is in fact not much different to that of *Harms et al.* [1992]. A tensor average for Franciscan sandstone in the Del Puerto Canyon shear zone (Table 1) shows that the maximum stretch direction did not involve any significant extension. We argue that the average direction of the "mylonitic lineations" of *Harms et al.* [1992] cannot be used to infer the direction of tectonic transport and that the low-strain SMT fabrics of the Franciscan sandstones cannot be compared to S-C fabrics, which are characteristic for high-strain mylonites deformed by crystal-plastic processes. Those mylonites usually have R_{XZ} values of >10 and up to 100 or even more.

[43] The average of the strain tensor from the proposed Del Puerto Canyon shear zone is $S_X : S_Y : S_Z = 1.05 : 0.99 : 0.95$, indicating plane strain. The strain-tensor average from all of our samples from Del Puerto Canyon is $S_X : S_Y : S_Z = 1.04 : 0.96 : 0.93$. The small volume strains can be

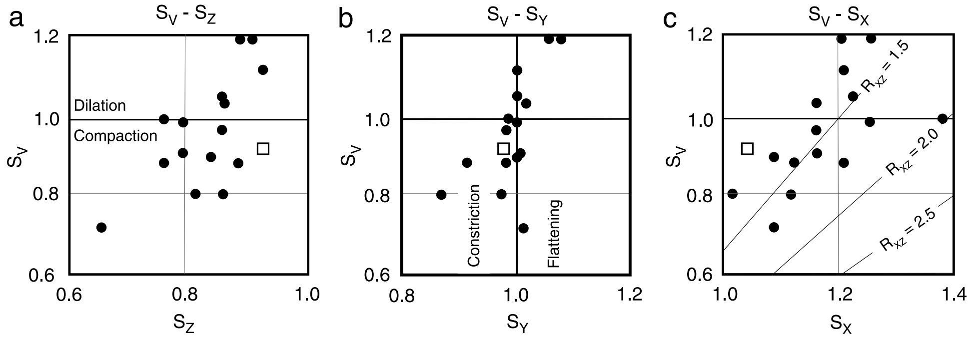

Figure 6. Finite-strain data plotted in (a) $S_V - S_Z$, (b) $S_V - S_Y$ and (c) $S_V - S_X$ diagram into which contours of R_{XZ} for the plane-strain case are projected; data points in $S_V - S_Y$ diagram are close to plane strain, average of strain tensor for all data plots in constrictional field close to plane-strain line. $S_V - S_Z$ diagram shows that relatively high aspect ratios in XZ section, which provide measure of cleavage intensity, do not correspond to large stretches in X when volume strains are considered. All absolute stretches show positive correlation with volume strain.

considered as a form of mass loss within the Franciscan accretionary wedge. We believe it is important to note that strain, and also rotation, in the proposed mylonite zone in the uppermost Franciscan is similar to strain and rotation from areas outside this zone. This supplies strong evidence for our conclusion that there is no high-strain zone at the contact between the Franciscan and the overlying Coast Range Ophiolite. We consider the contact between the Franciscan blueschists and the Coast Range Ophiolite as a late brittle fault that probably fits into the regional pattern of postmetamorphic top-west out-of-sequence thrusts within the Great Valley Group and the Franciscan [*Suppe*, 1973; *Cowan*, 1974; *Platt*, 1975; *Worrall*, 1981; *Wentworth et al.*, 1984; *Glen*, 1990; *Unruh et al.*, 1991, 1995; *Jachens et al.*, 1995; *Ring and Brandon*, 1994].

4.2. Implications for the Franciscan Subduction Complex

[44] Our results from Del Puerto Canyon are not different from those of other SMT-deformed Franciscan sandstones [*Ring and Brandon*, 1999; *Bolhar and Ring*, 2001]. The pattern of the principal finite-strain axes shows a considerable scatter for the entire Eastern Franciscan Belt. Individual samples from Franciscan sandstones show maximum extensional stretches between 0% and 52%. Tensor averages indicate that there was no extension associated with SMT deformation at the regional scale. The amounts and senses of internal rotation of these individual samples are also variable. The kinematic vorticity number is on average very small indicating a predominantly pure-shear style of deformation. Furthermore, *Ring and Brandon* [1999] showed that the variable vorticity at the local scale averages out. Models involving simple-shear deformation of the entire wedge are therefore not applicable to the Franciscan. Rather, the overall deformation in the Eastern Franciscan Belt can be approximated as a distributed, heterogeneous coaxial plane deformation accompanied by a negative volume strain.

[45] The lack of noncoaxial deformation and any extension in the Eastern Belt together with the lack of support for the proposed extensional mylonite zone in Del Puerto Canyon has profound implications for the exhumation of the Franciscan high-pressure rocks. There is no currently identifiable structure adjacent to or within the Franciscan subduction complex in California that could have accommodated large-scale normal slip. The important conclusion is that the Franciscan high-pressure rocks were not exhumed by normal faulting. In line with *Ring and Brandon* [1999], we propose that erosion was the dominant exhumation process. The required erosion rates of $\sim$0.4–0.8 km Myr^{-1} are not unusual for an orogenic setting. For instance, *Brandon and Vance* [1992] and *Brandon et al.* [1998] reported an average erosion rate of about 0.8 km Myr^{-1} for the Olympic Mountains forearc high associated with the modern Cascadia convergent margin.

Table 2. Comparison of Stretches and Axial Ratios Obtained From PDS and Mode Measurements of SMT Deformation on Quartz Grains and R_f/ϕ Analysis of Lithic Fragments[a]

		Stretches				Axial Ratios			
Sample	Method	S_X	S_Y	S_Z	S_V	R_{XY}	R_{YZ}	R_{XZ}	Γ_{oct}
P3/4	SMT	1.10	0.86	0.86	0.80	1.28	1.00	1.28	0.41
P3/4	R_f/ϕ	1.24	1.03	0.63	0.80	1.20	1.63	1.97	0.56
93-27a	SMT	1.09	0.78	0.77	0.65	1.40	1.01	1.42	0.33
93-27a	R_f/ϕ	1.17	1.04	0.50	0.65	1.13	2.08	2.34	0.42
96-57	SMT	1.12	0.82	0.74	0.68	1.37	1.11	1.51	0.36
96-57	R_f/ϕ	1.24	0.97	0.46	0.68	1.28	2.11	2.70	0.53

[a]Only sample P3/4 from Del Puerto Canyon had enough lithic fragments for R_f/ϕ work; stretches from R_f/ϕ results were recalculated for volume strain obtained from SMT strain of same sample (the relationship between deviatoric, S', and absolute stretches, S, is as follows: $S = S' \times S_V^{1/3}$; therefore principal stretches would be higher if calculated for constant volume).

[46] Our strain results do not only indicate that mylonitic extensional fabrics in Del Puerto Canyon do not exist, they are also inconsistent with the model of *Platt* [1986] according to which the Franciscan was a supercritically tapered wedge and that supercritical tapering triggered normal faulting. Taking the average of our strain measurements (Table 1), a residence time in the wedge of 35 Myr for the graywacke from Del Puerto Canyon, a burial depths of 30 km, coaxial deformation and a depth-dependent rate for ductile deformation, we calculate vertically averaged strain rates. Because the principal strain axes of the tensor average are all inclined, the vertical averaging changes the principal stretches. The horizontal principal stretch parallel to the $\sim$160°-striking Diablo Range becomes 0.96, that for across strike 0.98 and for vertical strain 0.98. Averaged strain rates are -3.3×10^{-17} s^{-1} for parallel-strike horizontal strain, -1.8×10^{-17} s^{-1} for across-strike horizontal strain, and -1.4×10^{-17} s^{-1} for vertical strain. The strain rates are related to volume loss and to the efficiency with which dissolved chemicals are advected away and are similar to the ones calculated by *Ring and Brandon* [1999] and *Bolhar and Ring* [2001] for other parts of the Eastern Franciscan Belt. These strain rates are orders of magnitude smaller than the 1×10^{-14} s^{-1} strain rates assumed by *Platt* [1986]. As a consequence of the slow strain rates and the high volume loss, ductile flow probably was not fast enough to significantly influence the stability of the wedge and to form a supercritically tapered wedge. In other words, our data imply that the wedge could not shorten horizontally fast, and hence could not have steepened up its surface slope. The fact that shortening was accompanied by volume loss has another important and interesting consequence. Even if a case was envisioned in which horizontal shortening was fast enough to steepen up the surface slope of the wedge, the volume loss would not necessarily change the wedge geometry into a supercritical configuration triggering normal faulting.

[47] The summary of finite-strain data from subduction-related accretionary wedges by *Brandon and Ring* [1998] indicates that the Franciscan wedge is not different to other circum-Pacific accretionary wedges, which are all characterized by small strain rates of the order of 1×10^{-16} s^{-1}. From this *Brandon and Ring* [1998] concluded that the stability of most subduction-related wedges is probably not influenced by viscous ductile mechanisms.

5. Closing Remarks

[48] The most important conclusion we draw from our study is that an important piece of evidence for extensional deformation in the Franciscan subduction complex, the proposed extensional mylonite zone in the uppermost Franciscan in Del Puerto Canyon, does not exist. There is no currently identifiable structure adjacent to or within the Franciscan in California that could have accommodated large-scale normal slip. Detailed work shows that strains in the Franciscan subduction complex are in general small and deformation is largely coaxial. As a consequence of the slow strain rates and the volume loss, ductile flow probably was not fast enough to form a supercritically tapered wedge.

[49] **Acknowledgments.** Funded by the Deutsche Forschungsgemeinschaft (Ri 538/8). We thank the private landowners in Del Puerto Canyon for their cooperation and the rangers of Frank Raines Park for their hospitality and logistic support. We thank John Wheeler for his helpful review and Doug Walker and Brian Wernicke for editorial support. An anonymous reviewer also commented on the manuscript.

References

Bailey, E. H., W. P. Irwin, and D. L. Jones (1964), Franciscan and related rocks, and their significance in the geology of western California, *Bull. Calif. Div. Mines Geol.*, *183*, 1–177.

Bartow, J. A., and T. H. Nilsen (1990), Review of the Great Valley sequence, eastern Diablo Range and northern San Joaquin Valley, central California, in *Structure, Stratigraphy and Hydrocarbon Occurrences of the San Joaquin Basin, California*, edited by J. G. Kuespert and S. A. Reid, pp. 253–265, Pac. Sect., Soc. of Econ. Paleontol. and Mineral., Bakersfield, Calif.

Bauder, J. M., and J. G. Liou (1979), Tectonic outlier of Great Valley sequence in Franciscan terrane, Diablo Range, California, *Geol. Soc. Am. Bull.*, *90*, 561–568.

Berkland, J. O., L. A. Raymond, J. C. Kramer, E. M. Moores, and M. O'Day (1972), What is Franciscan?, *AAPG. Bull.*, *56*, 2295–2302.

Berthé, D., P. Choukroune, and P. Jeguzo (1979), Orthogneiss, mylonite and non-coaxial deformation of granites, *J. Struct. Geol.*, *1*, 31–42.

Blake, M. C., Jr. (1981), Geologic transect of the northern Diablo Range, California, in *Upper Mesozoic Franciscan Rocks and Great Valley Sequence, Central Coast Ranges, California*, edited by V. Frizzell, pp. 35–43, Pac. Sect., Soc. of Econ. Paleontol. and Mineral., Los Angeles, Calif.

Blake, M. C., Jr., A. S. Jayko, R. J. McLaughlin, and M. B. Underwood (1988), Metamorphic and tectonic evolution of the Franciscan Complex, northern California, in *Metamorphism and Crustal Evolution of the Western United States*, edited by W. G. Ernst, pp. 1036–1059, Prentice-Hall, Old Tappan, N. J.

Bolhar, R., and U. Ring (2001), Deformation history of the Yolla Bolly terrane at Leech Lake Mountain, Eastern belt, Franciscan subduction complex, California Coast Ranges., *Geol. Soc. Am. Bull.*, *113*, 181–195.

Boyer, S. E., and D. Elliott (1982), Thrust systems, *AAPG Bull.*, *66*, 1196–1230.

Brandon, M. T. (1995), Analysis of geologic strain data in strain-magnitude space, *J. Struct. Geol.*, *17*, 1375–1385.

Brandon, M. T., and U. Ring (1998), Viscous flow and exhumation in Franciscan-like wedges, *Geol. Soc. Am. Abstr. Programs*, *31*(6), 40.

Brandon, M. T., and J. A. Vance (1992), Tectonic evolution of the Cenozoic Olympic subduction complex, Washington State, as deduced from fission track ages for detrital zircons, *Am. J. Sci.*, *292*, 565–636.

Brandon, M. T., D. S. Cowan, and J. G. Feehan (1994), Fault-zone structures and solution-mass-transfer cleavage in Late Cretaceous nappes, San Juan Islands, Washington, in *Geologic Field Trips in the Pacific Northwest*: *Geological Society of America 1994 Annual Meeting*, vol. 2L, edited by D. A. Swanson and R. A. Haugerud, pp. 1–19. Dep. of Geol. Sci., Univ. of Wash., Seattle.

Brandon, M. T., M. K. Roden-Tice, and J. I. Garver (1998), Late Cenozoic exhumation of the Cascadia accretionary wedge in the Olympic Mountains, NW Washington State, *Geol. Soc. Am. Bull.*, *110*, 985–1009.

Cashman, S. M., and H. M. Kelsey (1990), Forearc uplift and extension, southern Hawke's Bay, New Zealand: Mid-Pleistocene to Present, *Tectonics*, *9*, 23–44.

Cobbold, P. R. (1977), Description and origin of banded deformation structures. I. Regional strain, local perturbations, and deformation bands, *Can. J. Earth Sci.*, *14*, 1721–1731.

Constenius, K. N., R. A. Johnson, W. R. Dickinson, and T. A. Williams (2000), Tectonic evolution of the Jurassic-Cretaceous Great Valley forearc, California: Implications for the Franciscan thrust-wedge hypothesis, *Geol. Soc. Am. Bull.*, *112*, 1703–1723.

Cowan, D. S. (1974), Deformation and metamorphism of the Franciscan subduction zone complex northwest of Pacheco Pass, California, *Geol. Soc. Am. Bull.*, *85*, 1623–1634.

Cowan, D. S., and R. L. Bruhn (1992), Late Jurassic to early Late Cretaceous geology of the Cordillera, U.S., in *The Geology of North America*, vol. G3, *The Cordilleran Orogen: Conterminous U.S.*, edited by B. C. Burchfiel, P. W. Lipman, and M. L. Zoback, pp. 169–203, Geol. Soc. of Am., Boulder, Colo.

Cowan, D. S., and B. M. Page (1975), Recycled material in Franciscan melange west of Paso Robles, California, *Geol. Soc. Am. Bull.*, *86*, 1089–1095.

Deckert, H., and M. T. Brandon (2004), Shear coupling at subduction zones—Implications from X-ray texture goniometry on phyllosilicate-rich rocks from the Torlesse subduction wedge, New Zealand, *J. Struct. Geol.*, in press.

Deckert, H., U. Ring, and N. Mortimer (2002), Tectonic significance of Cretaceous bivergent extensional shear zones in the Torlesse accretionary wedge, central Otago Schist, New Zealand, *N. Z. J. Geol. Geophys.*, *45*, 537–547.

Dickinson, W. R., R. W. Ojakangas, and R. J. Stewart (1969), Burial metamorphism of the late Mesozoic Great Valley sequence, Cache Creek, California, *Geol. Soc. Am. Bull.*, *80*, 519–526.

Dickinson, W. R., R. V. Ingersoll, D. S. Cowan, K. P. Helmold, and C. A. Suczeki (1982), Provenance of Franciscan greywackes in coastal California, *Geol. Soc. Am. Bull.*, *93*, 95–107.

Dumitru, T. A. (1989), Constraints on uplift in the Franciscan Subduction Complex from apatite fission track analysis, *Tectonics*, *8*, 197–220.

Ernst, W. G. (1965), Mineral parageneses in Franciscan metamorphic rocks, Panoche Pass, California, *Geol. Soc. Am. Bull.*, *76*, 879–914.

Ernst, W. G. (1987), Jadeitized Franciscan metamorphic rocks of the Pacheco Pass-San Luis Reservoir area, central California Coast Ranges, in *Geological Society of America Centennial Field Guide–Cordilleran Section*, vol. 57, pp. 245–250, Geol. Soc. of Am., Boulder, Colo.

Ernst, W. G. (1992), Response to R. H. Grapes, *N. Z. J. Geol. Geophys.*, *35*, 385–387.

Ernst, W. G. (1993), Metamorphism of Franciscan tectonostratigraphic assemblage, Pacheco Pass area, east-central Diablo Range, California Coast Ranges, *Geol. Soc. Am. Bull.*, *105*, 618–636.

Evarts, R. C. (1977), The Geology and petrology of the Del Puerto ophiolite, Diablo Range, central California Coast Ranges, in *North American Ophiolites*, edited by R. G. Coleman and W. P. Irwin, *Bull. Oreg. Dep. Geol. Miner. Ind.*, *95*, 121–139.

Fassoulas, C., A. Kilias, and D. Mountrakis (1994), Postnappe stacking extension and exhumation of high-pressure/low-temperature rocks in the island of Crete, Greece, *Tectonics*, *13*, 127–138.

Feehan, J. G., and M. T. Brandon (1999), Contribution of ductile flow to exhumation of low-temperature, high-pressure metamorphic rocks: San Juan-Cascade Nappes, NW Washington State, *J. Geophys. Res.*, *104*, 10,883–10,901.

Fisher, D. M., and S. L. Brantley (1992), Models of quartz overgrowth and vein formation: Deformation and episodic fluid flow in an ancient subduction zone, *J. Geophys. Res.*, *97*, 20,043–20,061.

Glen, R. A. (1990), Formation and thrusting in some Great Valley rocks near the Franciscan Complex, California, and implications for the tectonic wedging hypothesis, *Tectonics*, *9*, 1451–1477.

Harms, T., A. S. Jayko, and M. C. Blake Jr. (1992), Kinematic evidence for extensional unroofing of the Franciscan Complex along the Coast Range fault zone, northern Diablo Range, California, *Tectonics*, *11*, 228–241.

Ingersoll, R. V. (1978), Paleogeography and paleotectonics of the late Mesozoic forearc basin of northern and central California, in *Mesozoic Paleogeography of the Western United States*, *Pacific Coast Paleogeography Symposium 2, April 26, 1978*, edited by D. G. Howell and K. A. McDougall, pp. 471–482, Pac. Sect., Soc. of Econ. Paleontol. and Mineral., Los Angeles, Calif.

Ingersoll, R. V. (1979), Evolution of the Late Cretaceous forearc basin, northern and central California, *Geol. Soc. Am. Bull.*, *90*, 813–826.

Irwin, W. P. (1960), Geologic reconnaissance of the northern Coast Ranges and Klamath Mountains, California, *Bull. Calif. Div. Mines Geol.*, *179*, 1–80.

Jachens, R. C., A. Griscom, and C. W. Roberts (1995), Regional extent of Great Valley basement west of the Great Valley, California: Implications for extensive tectonic wedging in the California Coast Ranges, *J. Geophys. Res.*, *100*, 12,769–12,790.

Jayko, A. S., M. C. Blake Jr., and T. Harms (1987), Attenuation of the Coast Range Ophiolite by extensional faulting, and nature of the Coast Range "thrust," California, *Tectonics*, *6*, 475–488.

Kamb, W. B. (1959), Ice petrofabric observations from Blue Glacier, Washington, in relation to theory and experiment, *J. Geophys. Res.*, *64*, 1891–1909.

Küster, M., and B. Stöckhert (1997), Density changes of fluid inclusions in high-pressure/low-temperature metamorphic rocks from Crete: A thermobarometric approach to the creep strength of host minerals, *Lithos*, *41*, 151–167.

Maddock, M. E. (1964), Geology of the Mt. Boardman Quadrangle, Santa Clara and Stanislaus counties, California, *Map Sheet 3*, Calif. Div. of Mines and Geol., San Francisco, Calif.

Massone, H.-J., and W. Schreyer (1987), Phengite geobarometry based on the limiting assemblage with K-feldspar, phlogopite, and quartz, *Contrib. Mineral. Petrol.*, *96*, 212–224.

Mattinson, J. M., and L. M. Echevirra (1980), Ortigalita Peak gabbro, Franciscan Complex: U-Pb ages of intrusion and high-pressure–low-temperature metamorphism, *Geology*, *8*, 589–593.

Nadai, A. (1963), *Theory of Flow and Fracture of Solids*, vol. 2, McGraw-Hill, New York.

Page, B. M., and L. T. Tabor (1967), Chaotic structure and decollement in Cenozoic rocks near Stanford University, California, *Geol. Soc. Am. Bull.*, *78*, 1–12.

Pettinga, J. R. (1982), Upper Cenozoic structural history, coastal southern Hawke's Bay, New Zealand, *N. Z. J. Geol. Geophys.*, *25*, 149–191.

Platt, J. P. (1975), Metamorphic and deformational processes in the Franciscan Complex, California: Some insights from the Catalina schist terrane, *Geol. Soc. Am. Bull.*, *86*, 1337–1347.

Platt, J. P. (1986), Dynamics of orogenic wedges and the uplift of high-pressure metamorphic rocks, *Geol. Soc. Am. Bull.*, *97*, 1037–1053.

Ramsay, J. G., and M. I. Huber (1983), *The Techniques of Modern Structural Geology*, vol. 1, Strain Analysis, 307 pp., Academic, San Diego, Calif.

Ring, U. (1995), Horizontal contraction or horizontal extension: Heterogeneous Late Eocene and Early Oligocene general shearing during blueschist- and greenschist-facies metamorphism at the Pennine-Austroalpine boundary zone in the Western Alps, *Geol. Rundsch.*, *84*, 843–859.

Ring, U. (1996), Kinematic analysis of heterogeneous brittle deformation at the Coast Range fault zone and ductile strain and mass loss in the Eastern Franciscan belt (Franciscan subduction complex, U.S.A.): Implications for the exhumation of high-pressure/low-temperature metamorphic rocks, Habilitation thesis, 164 pp., Univ. Mainz, Germany.

Ring, U., and M. T. Brandon (1994), Kinematic data for the Coast Range fault zone and implications for the exhumation of the Franciscan Subduction Complex, *Geology*, *22*, 735–738.

Ring, U., and M. T. Brandon (1999), Ductile strain and mass loss in the Franciscan subduction complex: Implications for exhumation processes in accretionary wedges, in *Exhumation Processes: Normal Faulting, Ductile Flow and Erosion*, edited by U. Ring et al., *Geol. Soc. Spec. Publ.*, *154*, 55–86.

Ring, U., M. T. Brandon, S. D. Willett, and G. S. Lister (1999), Exhumation processes, in *Exhumation Processes: Normal Faulting, Ductile Flow and Erosion*, edited by U. Ring et al., *Geol. Soc. Spec. Publ.*, *154*, 1–27.

Ring, U., P. W. Layer, and T. Reischmann (2001a), Miocene high-pressure metamorphism in the Cyclades and Crete, Aegean Sea, Greece: Evidence for large-magnitude displacement on the Cretan detachment, *Geology*, *29*, 395–398.

Ring, U., M. T. Brandon, and A. Ramthun (2001b), Solution-mass-transfer deformation adjacent to the Glarus thrust, with implications for the tectonic evolution of the Alpine wedge in eastern Switzerland, *J. Struct. Geol.*, *23*, 1491–1505.

Suppe, J. (1973), Geology of the Leech Lake Mountain-Ball Mountain region, California: A cross-section of the northeastern Franciscan belt and its tectonic implications, *Univ. Calif. Publ. Geol. Sci.*, *107*, 82 pp.

Suppe, J., and R. L. Armstrong (1972), Potassium-argon dating of Franciscan metamorphic rocks, *Am. J. Sci.*, *272*, 217–233.

Tagami, T., and T. A. Dumitru (1996), Provenance and thermal history of the Franciscan accretionary complex: Constraints from zircon fission track thermochronology, *J. Geophys. Res.*, *101*, 1353–1364.

Thomson, S. N., B. Stöckhert, and M. A. Brix (1999), Miocene high-pressure metamorphic rocks of Crete, Greece: Rapid exhumation by buoyant escape, in *Exhumation Processes: Normal Faulting, Ductile Flow and Erosion*, edited by U. Ring et al., *Geol. Soc. Spec. Publ.*, *154*, 87–108.

Unruh, J. R., V. R. Ramirez, S. P. Phipps, and E. M. Moores (1991), Tectonic wedging beneath forearc basins: Ancient and modern examples from California and the Lesser Antilles, *GSA Today*, *1*, 185–190.

Unruh, J. R., B. A. Loewen, and E. M. Moores (1995), Progressive arcward contraction of a Mesozoic-Tertiary fore-arc basin, southwestern Sacramento Valley, California, *Geol. Soc. Am. Bull.*, *107*, 38–53.

Wakabayashi, J. (1992), Nappes, tectonics of oblique plate convergence, and metamorphic evolution related to 140 Ma of continuous subduction, Franciscan Complex, California, *J. Geol.*, *100*, 19–40.

Walcott, R. I. (1987), Geodetic strain and the deformational history of the North Island of New Zealand during the late Cainozoic, *Philos. Trans. R. Soc. London, Ser. A*, *321*, 163–181.

Wentworth, C. W., M. C. Blake, D. L. Jones, A. W. Walter, and M. D. Zoback (1984), Tectonic wedging associated with emplacement of the Franciscan assemblage, California Coast Ranges, in *Franciscan Geology of Northern California*, edited by M. C. Blake Jr., pp. 163–173, Pac. Sect., Soc. of Econ. Paleontol. and Mineral., Los Angeles, Calif.

Wheeler, J., and R. W. H. Butler (1993), Evidence for extension in the western Alpine orogen: The contact between the oceanic Piemonte and overlying continental Sesia units, *Earth Planet. Sci. Lett.*, *117*, 457–474.

Wheeler, J., and R. W. H. Butler (1994), Criteria for identifying structures related to true crustal extension in orogens, *J. Struct. Geol.*, *16*, 1023–1027.

Worrall, D. M. (1981), Imbricate low-angle faulting in uppermost Franciscan rocks, South Yolla Bolly area, northern California, *Geol. Soc. Am. Bull.*, *92*, 703–729.

P. P. Richter and U. Ring, Institut für Geowissenschaften, Johannes Gutenberg-Universität, D-55099 Mainz, Germany. (ring@uni-mainz.de)